

## The Ozonation of Silanes and Germanes: An Experimental and Theoretical Investigation

Janez Cerkovnik,<sup>†</sup> Tell Tuttle,<sup>‡§</sup> Elfi Kraka,<sup>‡</sup> Nika Lendero,<sup>†</sup>  
Božo Plesničar,<sup>\*†</sup> and Dieter Cremer<sup>\*‡</sup>

Contribution from the Department of Chemistry, Faculty of Chemistry and Chemical Technology, University of Ljubljana, P.O. Box 537, 1000 Ljubljana, Slovenia, and the Departments of Chemistry and Physics, University of the Pacific, 3601 Pacific Avenue, Stockton, California 95211, USA

Received November 28, 2005; E-mail: bozo.plesnicar@fkkt.uni-lj.si; dcremer@pacific.edu

**Abstract:** Ozonation of various silanes and germanes produced the corresponding hydrotrioxides, R<sub>3</sub>-SiOOOH and R<sub>3</sub>GeOOOH, which were characterized by <sup>1</sup>H, <sup>13</sup>C, <sup>17</sup>O, and <sup>29</sup>Si NMR, and by infrared spectroscopy in a two-pronged approach based on measured and calculated data. Ozone reacts with the E–H (E = Si, Ge) bond via a concerted 1,3-dipolar insertion mechanism, where, depending on the substituents and the environment (e.g., acetone-*d*<sub>6</sub> solution), the H atom transfer precedes more and more E–O bond formation. The hydrotrioxides decompose in various solvents into the corresponding silanols/germanols, disiloxanes/digermoxanes, singlet oxygen (O<sub>2</sub>(<sup>1</sup>Δ<sub>g</sub>)), and dihydrogen trioxide (HOOOH), where catalytic amounts of water play an important role as is indicated by quantum chemical calculations. The formation of HOOOH as a decomposition product of organometallic hydrotrioxides in acetone-*d*<sub>6</sub> represents a new and convenient method for the preparation of this simple, biochemically important polyoxide. By solvent variation, singlet oxygen (O<sub>2</sub>(<sup>1</sup>Δ<sub>g</sub>)) can be generated in high yield.

### Introduction

Reactions of ozone with saturated organic substrates leading to organic hydrotrioxides and dihydrogen trioxide are at the focus of current research, especially because of their relevance to the toxicity of ozone for the human body.<sup>1,2</sup> Although the involvement of hydrotrioxides, ROOOH, in the reaction of ozone with C–H bonds has already been well documented, the ozonation of organometallic hydrides, such as silanes and germanes, and the potential involvement of the corresponding hydrotrioxides in these reactions were much less explored. These polyoxides have already been proposed in the past as unstable intermediates in the reaction of ozone with various silanes.<sup>3</sup> More recently, Corey et al. have presented evidence that

triethylsilyl hydrotrioxide (Et<sub>3</sub>SiOOOH), generated by the low-temperature ozonation of triethylsilane, is an excellent source of singlet oxygen (O<sub>2</sub>(<sup>1</sup>Δ<sub>g</sub>)).<sup>4</sup> Et<sub>3</sub>SiOOOH was also demonstrated to react with electron-rich olefins to give dioxetanes that react intramolecularly with a keto group in the presence of *tert*-butyldimethylsilyl triflate to afford 1,2,4-trioxanes, some of them with a very potent antimalarial activity (Posner trioxane synthesis).<sup>5</sup> However, no unambiguous direct spectroscopic evidence for the existence of this hydrotrioxide was presented at that time.

We have already characterized dimethylphenylsilyl hydrotrioxide as a reactive intermediate in the low-temperature ozonation of dimethylphenylsilane and suggested that dihydrogen trioxide (HOOOH) might be one of the products formed during its decomposition.<sup>6</sup> Here we now report that the formation of HOOOH (among other products) is indeed the characteristic feature of the decomposition of various silyl as well as germyl hydrotrioxides, generated by the low-temperature ozonation of the corresponding silanes and germanes. This represents still another convenient method for the preparation of HOOOH.<sup>2</sup> The results of detailed experimental and theoretical studies of the NMR and IR spectral characterization of the polyoxides

<sup>†</sup> University of Ljubljana.

<sup>‡</sup> University of the Pacific.

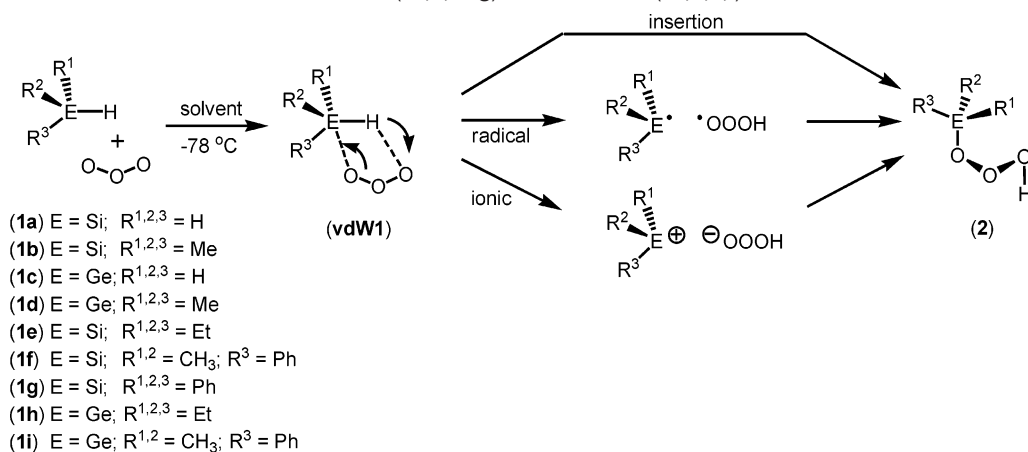
<sup>§</sup> Current address: Max-Planck-Institut für Kohlenforschung, Kaiser-Wilhelm-Platz 1, Mülheim an der Ruhr, 45470 Germany.

- (1) (a) Plesničar, B.; Tuttle, T.; Cerkovnik, J.; Koller, J.; Cremer, D. *J. Am. Chem. Soc.* **2003**, *125*, 11553. (b) Nyffeler, P. T.; Boyle, N. A.; Eltepu, L.; Wong, C.-H.; Eschenmoser, A.; Lerner, R. A.; Wentworth, P., Jr. *Angew. Chem., Int. Ed.* **2004**, *43*, 4656. (c) Tuttle, T.; Cerkovnik, J.; Plesničar, B.; Cremer, D. *J. Am. Chem. Soc.* **2004**, *126*, 16093.
- (2) (a) Engdahl, A.; Nelander, B. *Science* **2002**, *295*, 482. (b) Wentworth, P., Jr.; Jones, L. H.; Wentworth, A. D.; Zhu, X. Y.; Larsen, N. A.; Wilson, I. A.; Xu, X.; Goddard, W. A., III; Janda, K. D.; Eschenmoser, A.; Lerner, R. A. *Science* **2001**, *293*, 1806. (c) Suma, K.; Sumiyoshi, Y.; Endo, Y. *J. Am. Chem. Soc.* **2005**, *127*, 14998. (d) For a review on HOOOH, see: Plesničar, B. *Acta Chim. Slov.* **2005**, *52*, 1.
- (3) (a) Spialter, L.; Pazdernik, L.; Bernstein, S.; Swansiger, W. A.; Buell, G. R.; Freeburger, M. E. *J. Am. Chem. Soc.* **1971**, *93*, 5682. (b) Spialter, L.; Swansiger, W. A.; Pazdernik, L.; Freeburger, M. E. *J. Organomet. Chem.* **1971**, *27*, C25. (c) Spialter, L.; Swansiger, W. A. *J. Am. Chem. Soc.* **1968**, *90*, 2187. (d) Ouellette, R. J.; Marks, D. L. *J. Organomet. Chem.* **1968**, *11*, 407. (e) Spialter, L.; Pazdernik, L.; Bernstein, S.; Swansiger, W. A.; Buell, G. R.; Freeburger, M. E. *Adv. Chem. Ser.* **1972**, *112*, 65. (f) Alexandrov, Yu. A.; Tarunin, B. I. *J. Organomet. Chem.* **1982**, *238*, 125.

(4) Corey, E. J.; Mehrotra, M. M.; Khan, A. U. *J. Am. Chem. Soc.* **1986**, *108*, 2472.

(5) (a) Posner, G. H.; Weitzberg, M.; Nelson, W. M.; Murr, B. L.; Seliger, H. H. *J. Am. Chem. Soc.* **1987**, *109*, 278. (b) Posner, G. H.; Webb, K. S.; Nelson, W. M.; Kishimoto, T.; Seliger, H. H. *J. Org. Chem.* **1989**, *54*, 3252. (c) Posner, G. H.; Oh, C. H.; Milhous, W. K. *Tetrahedron Lett.* **1991**, *32*, 4235. (d) Hassner, A.; Stumer, C. *Organic Syntheses Based on Name Reactions*, 2nd ed.; Pergamon: Amsterdam, Boston, 2002; p 293.

(6) Plesničar, B.; Cerkovnik, J.; Koller, J.; Kovač, F. *J. Am. Chem. Soc.* **1991**, *113*, 4946.

**Scheme 1.** Possible Ozonation Mechanisms for Silanes (**1a,b,e–g**) and Germanes (**1c,d,h,i**)

under investigation as well as of the mechanism of their formation and decomposition are presented.

## Experimental Section

Instrumentation, materials (see also Scheme 1), ozonation procedures, product analysis, and methodology of kinetic studies are collected in the section Supporting Information.

The theoretical investigation focused on the study of the model systems: silane (**1a**), trimethylsilane (**1b**), germane (**1c**), and trimethylgermane (**1d**) (see Scheme 1) and was based on a variety of methods, including density functional theory (DFT),<sup>7</sup> Many Body Perturbation theory using the Møller Plesset Hamiltonian at second and fourth order (MP2 and MP4)<sup>8</sup> (for energy, geometry, and other property calculations), the polarizable continuum descriptions COSMO and PISA (for solvent effect calculations),<sup>9</sup> sum-over-states density functional perturbation theory (SOS-DFPT) based on the “individual gauge for localized orbitals” (IGLO) scheme<sup>10</sup> (NMR shift calculations), and the adiabatic vibrational mode analysis<sup>11</sup> (calculation and analysis of infrared spectra). Calculations were performed using the program packages COLGNE 2005<sup>12a</sup> and Gaussian 03.<sup>12b</sup> Details of the methods used, the calculation protocol, and the full references for the programs applied can also be found in the Supporting Information.

## Results and Discussion

**Ozonation of Silanes and Germanes (Experimental Results).** Ozonation of trimethylsilane (**1b**), triethylsilane (**1e**), dimethylphenylsilane (**1f**), or triphenylsilane (**1g**) (**1**, 0.1 ± 0.05M) (see Scheme 1) with ozone–oxygen or ozone–nitrogen

mixtures in various solvents (acetone-*d*<sub>6</sub>, methyl acetate, *tert*-butyl methyl ether, methylene chloride-*d*<sub>2</sub>, toluene-*d*<sub>8</sub>) at −78 °C produced the corresponding hydrotrioxide (**2**), characterized by the OOOH <sup>1</sup>H NMR absorption at δ 13.0 ± 1.0 ppm downfield from Me<sub>4</sub>Si in yields of 70–90%, as determined by <sup>1</sup>H NMR spectroscopy. The <sup>1</sup>H, <sup>13</sup>C, <sup>17</sup>O, and <sup>29</sup>Si NMR data of **2** are, together with those of some other silicon homologues, collected in Table 1. For selected segments of NMR and IR spectra of triethylsilyl hydrotrioxide (**2e**), see Figures 1 and 2 (see also Figure S1 for deuterated analogues in Supporting Information).

Similar observations were also made by studying low-temperature ozonation of triethylgermane (**1h**) and dimethylphenylgermane (**1i**) (0.01–0.05 M) in acetone-*d*<sub>6</sub>, methyl acetate, and *tert*-butyl methyl ether at −78 °C. The corresponding hydrotrioxides with characteristic OOOH <sup>1</sup>H NMR absorption at δ 13.0 ± 0.5 ppm downfield from Me<sub>4</sub>Si were formed in yields of 30–50%. The <sup>1</sup>H, <sup>13</sup>C, and <sup>17</sup>O NMR data of **2i,h** are collected in Table 1.

Still another OOOH absorption at δ 13.2 ± 0.3 ppm, corresponding to another polyoxide species with exchangeable protons (as determined by a relatively fast exchange with DOD at −60 °C), was observed in the <sup>1</sup>H NMR spectra. This absorption was assigned to dihydrogen trioxide (HOOOH), on the basis of <sup>17</sup>O NMR spectra of polyoxides that were highly enriched with <sup>17</sup>O.<sup>1a</sup>

### Ozonation of Silanes and Germanes (Theoretical Results).

The basic mechanism proposed for the ozonation of compounds **1a–d** (Scheme 1) followed the mechanism found for the ozonation of hydrocarbons.<sup>13</sup> However, contrary to the hydrocarbons, in the ozonation of silanes and germanes, the formation of complexes **vdW1a–d** (see Scheme 1) could not be confirmed. At the DFT level, the vdW structures found (listed in Tables 2 and 3) were no longer stable after BSSE (basis set superposition error) corrections had been included into the quantum chemical description. Also at the MP2 level of theory, the stabilization of potential vdW complexes was smaller than the changes caused by vibrational corrections. Considering the fact that the H atoms directly bonded to Si or Ge are negatively charged and that ozone has a dipole moment of just 0.53 (0.7 calculated) Debye,<sup>14</sup> other than weak dispersion interactions,

- (7) (a) Kohn, W.; Sham, L. *Phys. Rev. A* **1965**, *140*, 1133. For reviews on DFT, see for example: (b) Parr, R. G.; Yang, W. *International Series of Monographs on Chemistry 16: Density Functional Theory of Atoms and Molecules*; Oxford University Press: New York, 1989. (c) *Theoretical and Computational Chemistry, Vol. 2, Modern Density Functional Theory/A Tool for Chemistry*; Seminario, J. M., Politzer, P., Eds.; Elsevier: Amsterdam, 1995.
- (8) For a recent review, see: (a) Cremer, D. In *Encyclopedia of Computational Chemistry*; Schleyer, P. v. R., Allinger, N. L., Clark, T., Gasteiger, J., Kollman, P. A., Schaefer, H. F., III, Schreiner, P. R., Eds.; Wiley: Chichester, 1998; Vol. 3, p 1706. See also: (b) Møller, C.; Plesset, M. S. *Phys. Rev.* **1934**, *46*, 618.
- (9) (a) Miertus, S.; Scrocco, E.; Tomasi, J. *J. Chem. Phys.* **1981**, *55*, 117. (b) Barone, V.; Cossi, M.; Tomasi, J. *J. Chem. Phys.* **1997**, *107*, 3210. (c) Cammi, R.; Cossi, M.; Tomasi, J. *J. Chem. Phys.* **1996**, *104*, 4611. (d) Mennucci, B.; Tomasi, J. *J. Chem. Phys.* **1997**, *106*, 5151. (e) Tomasi, J.; Mennucci, B. In *Encyclopedia of Computational Chemistry*; Schleyer, P. v. R., Allinger, N. L., Clark, T., Gasteiger, J., Kollman, P. A., Schaefer, H. F., III, Schreiner, P. R., Eds.; Wiley: Chichester, 1998; Vol. 1, p 2547.
- (10) (a) Olsson, L.; Cremer, D. *J. Chem. Phys.* **1996**, *105*, 8995. (b) Olsson, L.; Cremer, D. *J. Phys. Chem.* **1996**, *100*, 16881.
- (11) Konkoli, Z.; Cremer, D. *Int. J. Quantum Chem.* **1998**, *67*, 1.
- (12) (a) Kraka, E.; Gräfenstein, J.; Filatov, M.; He, Y.; Gauss, J.; Wu, A.; Polo, V.; Olsson, L.; Konkoli, Z.; He, Z.; Cremer, D. *COLOGNE 2005*; University of the Pacific: Stockton, CA, 2005. (b) Frisch, M. J.; et al. *Gaussian 03*, revision C.01; Gaussian, Inc.: Wallingford, CT, 2004.

(13) Wu, A.; Cremer, D.; Plesničar, B. *J. Am. Chem. Soc.* **2003**, *125*, 9395.

(14) *CRC Handbook of Chemistry and Physics on CD-ROM*, 2000 version; Lide, D. R., Ed.; CRC Press LLC: Boca Raton, FL, 2000.

**Table 1.** Comparison of Selected  $^1\text{H}$ ,  $^{13}\text{C}$ ,  $^{29}\text{Si}$ , and  $^{17}\text{O}$  NMR Chemical Shifts for Some Hydrotrioxides of Silanes and Germanes (**2**), and Some of Their Analogues in Acetone- $d_6$  at  $-30\text{ }^\circ\text{C}^a$ 

	Species	$^1\text{H}$ NMR		$^{13}\text{C}$ NMR		$^{29}\text{Si}$ NMR	$^{17}\text{O}$ NMR
		$\text{R}_3\text{E}-\text{X}^b$	$\delta\text{CH}_3$	$\delta\text{E}-\text{X}$	$\delta\text{CH}_3$	$\delta\text{C}(1)^c$	$\delta\text{Si}$
<b>(1b)</b>	X = H		trimethylsilane				
	OH	0.074	3.94	2.00		-16.12	
	OOH	0.058	3.5–5.0	1.50		12.57	12.6
<b>(2b)</b>	O3O2O1H <sup>d</sup>	0.15	10.4	-1.48		24.85	
		0.23	13.48	-2.44		30.95	305 (O1) 434 (O2) 318 (O3)
<b>(1e)</b>	X = H		triethylsilane <sup>e</sup>				
	OH	0.70	4.20	15.0		-15.24	
	OOH	0.75	3.5–5.0	13.4		10.50	12.7
<b>(2e)</b>	O3O2O1H	0.82	10.3	11.2		23.45	
		0.95	13.48	10.5		29.64	305 (O1) 433 (O2) 319 (O3)
<b>(1f)</b>	X = H		dimethylphenylsilane				
	OH	0.30	4.40	-1.1	140.6	-16.95	
	O2O1H	0.32	4.5–5.5	3.1	143.5	3.30	22.0
<b>(2f)</b>	O3O2O1H	0.43	10.4	2.8	139.6	14.31	213 (O1) 265 (O2)
		0.55	13.45	2.7	138.5	17.31	303 (O1) 419 (O2) 320 (O3)
<b>(1h)</b>	X = H		triethylgermane <sup>e</sup>				
	OH	1.06	3.66	8.2			13.5
	O2O1H	1.07	4.5–5.0	8.4			221 (O1) 250 (O2)
<b>(2h)</b>	O3O2O1H	1.09	10.2				306 (O1) 435 (O2) 335 (O3)
		1.11	12.95	7.0			
<b>(1i)</b>	X = H		dimethylphenylgermane				
	OH	0.35	3.80	4.7	140.2		
	O2O1H	0.55	5.0–5.5	1.4			24.0
<b>(2i)</b>	O3O2O1H	0.70	10.6	-1.7	138.9		216 (O1) 264 (O2)
		0.84	13.06	-2.6	138.1		305 (O1) 420 (O2) 337 (O3)

<sup>a</sup> **2** = (0.07 ± 0.02) M. Chemical shifts in parts per million relative to the internal standard: tetramethylsilane ( $^1\text{H}$ ,  $^{13}\text{C}$ , and  $^{29}\text{Si}$  NMR) and  $\text{H}_2\text{O}$  ( $^{17}\text{O}$  NMR). <sup>b</sup> E = Si, Ge. <sup>c</sup> Chemical shift for C(1) atom in the phenyl ring. <sup>d</sup> Chemical shifts for **2b** were obtained at  $-50\text{ }^\circ\text{C}$ . <sup>e</sup>  $^1\text{H}$  NMR signals for the  $\text{CH}_2$  and  $\text{CH}_3$  groups appear as quartets and triplets, respectively.

binding between ozone and a silane (germane) molecule is either unlikely or unfavorable.

According to the calculated TS geometries **TS1(1a–d)** shown in Figure 3, the formation of the silyl hydrotrioxide (**2a**) occurs in a concerted fashion with the 1,3-insertion of ozone into the Si–H bond. This is obvious for **TS1(1a)** because both terminal O atoms of ozone are close to either H(Si) or Si atom (1.54 and 2.35 Å, respectively; Figure 3a). Also, the Si–H distance is lengthened from 1.48 to 1.62 Å, indicating the breaking of this bond. For the purpose of confirming the pericyclic insertion mechanism and distinguishing it from a H abstraction reaction caused by ozone, we carried out IRC (intrinsic reaction coordinate) calculations, which led indeed to  $\text{H}_3\text{SiOOOH}$  (**2a**) as the product. The activation enthalpy for the insertion reaction is fairly modest ( $\Delta H_{\text{act}}(\mathbf{1a}) = 10.7\text{ kcal/mol}$ ), although due to the large loss in entropy relative to the separated products, the Gibbs activation energy is twice as large ( $\Delta G_{\text{act}}(\mathbf{1a}) = 21.7\text{ kcal/mol}$ ). The product is formed in a strongly exothermic reaction ( $\Delta H_{\text{react}}(\mathbf{2a}) = -69.1\text{ kcal/mol}$ ).

For the purpose of testing the adequacy of the basis set in describing the ozone–silane reaction, all structures along the

reaction path of **1a** were reoptimized using the more complete 6-311++G(3df,3pd) basis set. The larger basis set led to little change in the reaction energetics (Table 2, values in parentheses); the activation enthalpy was increased relative to the 6-31G(d,p) results by 1.4 kcal/mol ( $\Delta H_{\text{act}} = 12.1\text{ kcal/mol}$ ), whereas the reaction enthalpy decreased by 1.8 to  $-71.0\text{ kcal/mol}$ . Since the structural and electronic changes are similar for all molecules investigated in this work, we can conclude that the moderate enthalpic differences and the conservation of the preferred reaction mechanism obtained with the larger basis set confirm the reliability of the smaller, 6-31G(d,p), basis set for the description of the reactions investigated in this work.

The substitution of silane to form trimethylsilane (**1b**) results in some changes in the TS of the insertion reaction (Figure 3b). The Si–H bond is lengthened to 1.69 Å. There is a closer contact with one of the terminal ozone oxygen atoms (1.29 Å), whereas the other terminal O atom is separated by 3.5 Å from the Si atom. This clearly reflects the steric screening of the Si atom by the methyl groups, which makes a two-pronged attack of ozone more difficult. One could assume that because of the steric screening of the Si atom the barrier increases or the

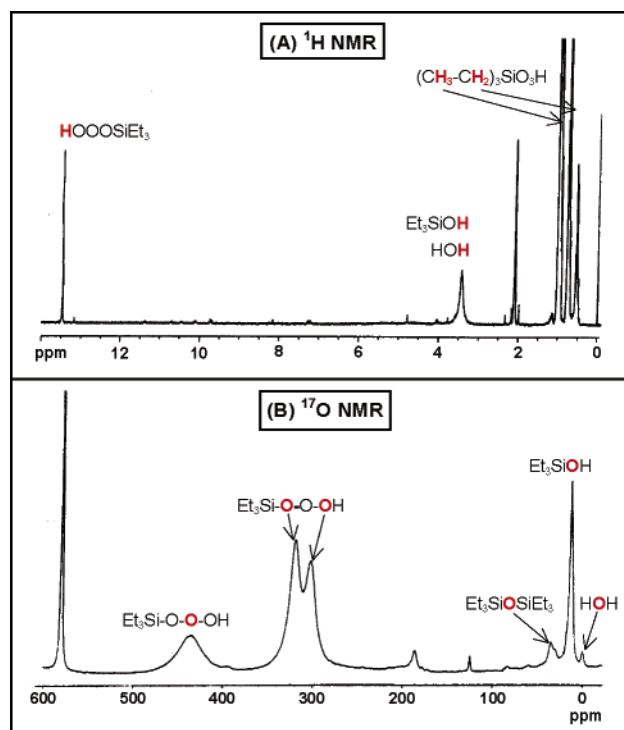


**Figure 1.** (A) <sup>1</sup>H and (B) <sup>17</sup>O NMR spectra of triethylsilyl hydrotrioxide (**2e**) at -30 °C, generated by the low-temperature ozonation of **1e** in acetone-*d*<sub>6</sub>.

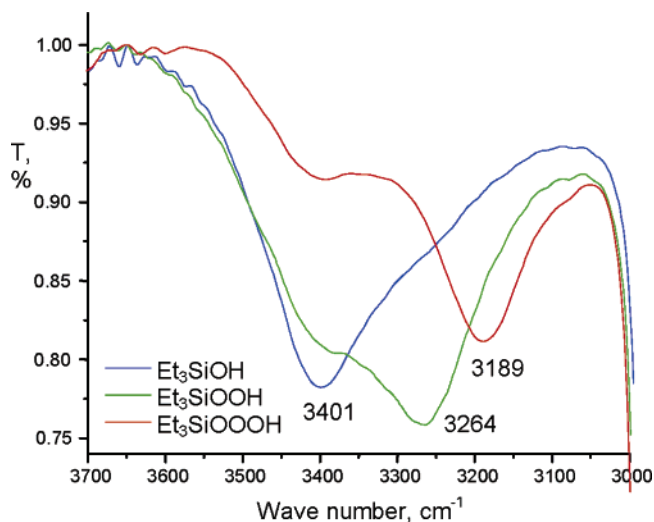


**Figure 2.** Segments of IR spectra of triethylsilyl hydrotrioxide (**2e**), and lower homologues (triethylsilanol and triethylsilyl hydroperoxide) in *tert*-butyl methyl ether at -65 °C (c(**2e**) = 1.0 ± 0.2 M).

insertion mechanism changes to a H abstraction reaction leading to the radical pair Me<sub>3</sub>Si•/•OOOH. However, IRC calculations reveal that the final product is still the hydrotrioxide (**2b**), simply because in the gas phase the homolytic splitting of the Si-H bond triggers the Si-O bond formation.<sup>15</sup>

Results indicate that, depending on the Si substituents, ozone insertion proceeds in a different fashion, with a H transfer either

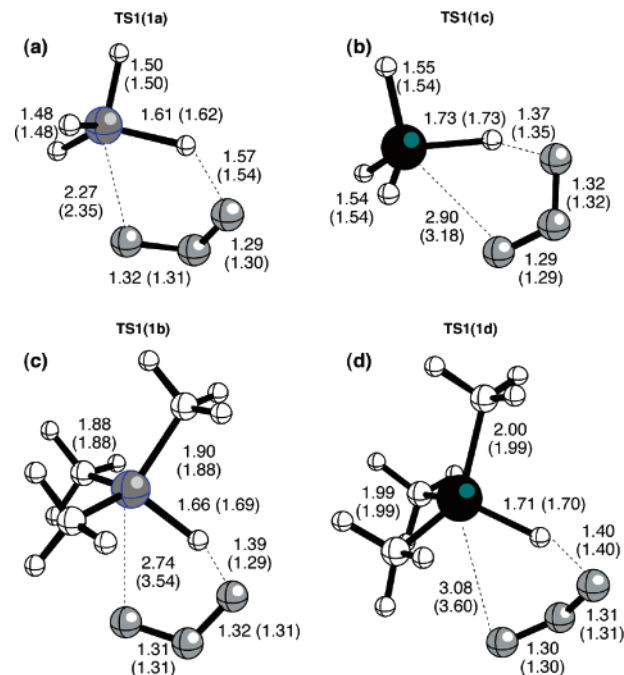


**Figure 3.** TS structures for the ozonation of compounds **1a**–**d**. Optimized gas-phase structures using the B3LYP functional and the 6-31G(d,p) basis set for all atoms except Ge, which was described with the SDD pseudo-potential and associated basis set. Values in parentheses correspond to the distances for the structures optimized using the CPCM solvent model with acetone as the solvent ( $\epsilon = 20.7$ ). Distances in Å. For details of the calculations, see the Supporting Information.

simultaneous to Si-O bond formation or a delayed Si-O bond formation. In the latter case, the barrier decreases rather than increases because Si-H bond cleavage is supported by the hyperconjugative and inductive effects of the three methyl groups that all withdraw electron density from the Si-H bond. These substituents are responsible for the magnitude of the reaction barrier because Si-O bond formation occurs relatively late in the exit channel of the concerted reaction.

Although in the gas phase the same type of product is always obtained, the difference in the insertion mechanisms may matter in solution (see below) considering the fact that the Me<sub>3</sub>Si•/•OOOH radical pair has an energy of just 2.3 kcal/mol relative to the reactants ( $\Delta H_{\text{rad}}(\mathbf{1b}) = 3.4$  kcal/mol), and by this it is 6.1 kcal/mol below the TS energy of 8.4 kcal/mol (Table 2).<sup>16</sup> The product of this reaction is again strongly stabilized below the reactants by -76.2 kcal/mol since the rather labile ozone  $\pi$ -bonds are converted into the polar (and thereby stabilized) Si-O and O-H single bonds.

The ozonation of both germane (**1c**) and trimethylgermane (**1d**) also follows an insertion mechanism with early O-H and late Ge-O bond formation as described for **1b** ( $\Delta H_{\text{act}}(\mathbf{1c}) = 10.9$ ;  $\Delta H_{\text{act}}(\mathbf{1d}) = 6.4$  kcal/mol; Table 2). Germane **1c** behaves differently than silane **1a**, which is not caused by steric screening but by the different polarity of the Ge-H bond compared to that of the Si-H bond. It has been demonstrated<sup>17</sup> that, contrary

(15) Pryor et al. have already discussed the possibility that in the ozonation of various saturated organic substrates (hydrocarbons, alcohols, ethers) a concerted insertion mechanism with the transition state having contributions from radical or ionic resonance forms might be operative in these oxidations. (a) Giamalva, D. H.; Church, D. F.; Pryor, W. A. *J. Am. Chem. Soc.* **1986**, *108*, 7678. (b) Giamalva, D. H.; Church, D. F.; Pryor, W. A. *J. Org. Chem.* **1988**, *53*, 3429. See also: (c) Hellman, T. M.; Hamilton, G. A. *J. Am. Chem. Soc.* **1974**, *96*, 1530.

(16) (a) The calculated activation energy of 8.4 kcal/mol for the ozonation of trimethylsilane (**1b**) is in excellent agreement with that reported for the ozonation of triethylsilane (**1e**) in CCl<sub>4</sub> (8.0 kcal/mol).<sup>3f</sup> (b) Considerable Si-H bond breaking in the transition state is indicated by a large kinetic isotope effect; i.e.,  $k_{\text{H}}/k_{\text{D}} = 6.9$ , for the ozonation of (*n*-C<sub>4</sub>H<sub>9</sub>)<sub>3</sub>SiH(D).<sup>3b</sup> (c) The Hammett  $\rho$  value of -1.43 was reported for the ozonation of dimethylphenylsilanes.<sup>3d</sup> (17) Giju, K. T.; De Proft, F.; Geerlings, P. *J. Phys. Chem. A* **2005**, *109*, 2925.

**Table 2.** Reaction Energies for the Gas-Phase-Optimized Ozonation of Silanes and Germanes (**1a–d**)<sup>a</sup>

molecule	$\Delta E$	$\Sigma ZPE$	$\Delta H$	$\Sigma S$	$\Delta G$	$\mu$
<b>1a</b>	-517.29447	24.23	-517.24795	110.72	-517.30056	0, 0.62
<b>vdW1a</b>	0.25 (0.01)	24.79 (24.48)	0.91 (1.19)	88.27 (103.68)	7.60 (3.26)	0.96 (0.66)
<b>TS1(1a)</b>	11.14 (12.74)	24.72 (24.28)	10.70 (12.06)	73.87 (76.02)	21.68 (22.37)	0.73 (1.06)
H <sub>3</sub> Si <sup>+</sup> + HOOO <sup>-</sup>	174.77 (155.22)	23.82 (23.49)	175.10 (155.35)	116.89 (117.69)	173.26 (153.24)	0, 0.60 (0, 0.98)
H <sub>3</sub> Si <sup>*</sup> + HOOO <sup>*</sup>	0.49 (1.09)	24.52 (24.35)	1.19 (1.71)	116.86 (117.15)	-0.64 (-0.24)	0.03, 1.22 (0.06, 1.13)
<b>2a</b>	-72.9 (-74.77)	28.78 (28.69)	-69.14(-70.97)	75.07 (75.45)	-58.52(-60.49)	2.90 (2.71)
<b>1b</b>	-635.28675	79.57	-635.14764	138.32	-635.21336	0, 0.62
<b>vdW1b</b>	0.54	79.98	1.71	117.96	7.78	0.16
<b>TS1(1b)</b>	8.42	78.57	7.34	104.45	17.44	2.64
Me <sub>3</sub> Si <sup>+</sup> + HOOO <sup>-</sup>	131.73	78.58	131.81	153.12	127.40	0, 0.60
Me <sub>3</sub> Si <sup>*</sup> + HOOO <sup>*</sup>	2.26	80.25	3.36	146.04	1.06	0.67, 1.22
<b>2b</b>	-79.48	83.00	-76.18	101.46	-65.19	3.59
<b>1c</b>	-231.59673	22.73	-231.55251	113.85	-231.60660	0, 0.62
<b>vdW1c</b>	3.74 (0.01)	23.17 (22.90)	4.37 (0.60)	93.02 (102.68)	10.58 (3.91)	0.90 (0.66)
<b>TS1(1c)</b>	11.93 (9.25)	22.27 (22.24)	10.95 (8.25)	80.68 (80.91)	20.84 (18.05)	1.46 (1.70)
H <sub>3</sub> Ge <sup>+</sup> + HOOO <sup>-</sup>	161.36 (139.57)	22.72 (22.73)	162.07 (140.36)	117.76 (120.72)	160.90 (138.29)	0, 0.60 (0, 0.98)
H <sub>3</sub> Ge <sup>*</sup> + HOOO <sup>*</sup>	-9.37 (-8.27)	23.41 (23.30)	-8.30 (-7.26)	117.80 (118.14)	-9.48 (-8.56)	0.06, 1.22 (0.15, 1.13)
<b>2c</b>	-57.6 (-62.68)	26.92(26.96)	-54.01(-58.97)	79.35(79.42)	-43.72(-48.73)	1.59 (1.56)
<b>1d</b>	-349.56875	78.56	-349.43064	143.53	-349.49883	0, 0.62
<b>vdW1d</b>	3.77	79.03	4.95	120.92	11.69	0.18
<b>TS1(1d)</b>	7.40	77.57	6.44	111.02	16.13	2.74
Me <sub>3</sub> Ge <sup>+</sup> + HOOO <sup>-</sup>	122.28	78.49	123.13	157.93	118.840	0, 0.60
Me <sub>3</sub> Ge <sup>*</sup> + HOOO <sup>*</sup>	-8.93	79.67	-7.45	150.82	-9.62	0.46, 1.22
<b>2d</b>	-67.20	82.01	-63.65	109.74	-53.58	2.03

<sup>a</sup> The energies, enthalpies, and free energies are given in kcal mol<sup>-1</sup>. The entropy is in e.u., and the dipole moment is in debye. All calculations were performed with B3LYP. The 6-31G(d,p) basis set was used for all atoms (values in parentheses calculated with 6-311++G(3df,3pd) basis set) except Ge, which was treated with the SDD pseudopotential (for details, see Supporting Information).

to the normal behavior of atoms in a group of the periodic table, Ge as the element with the larger atomic number is somewhat less electropositive (more electronegative) than Si, which leads to a reduced charge transfer from Ge to H (see NBO charges in Figure 4). The Ge–H bond is less polar and by this weaker than the Si–H bond. This effect is enhanced by the smaller overlap between a 4pσ(Ge) and the 1s(H) orbital compared to that between the 3pσ(Si) and the 1s(H) orbital. Hence, Ge–H is more prone to homolytic (or heterolytic) bond cleavage than Si–H (see Table 2). This is confirmed by the activation enthalpies calculated with the larger basis set<sup>18</sup> (**1a**, 12.1; **1c**, 8.2 kcal/mol; the smaller basis set is not sensitive to this difference) and by the geometry of **TS1(1c)**, which identified early Ge–H bond breakage. Methyl screening of Ge leads to another reduction of the activation enthalpy (6.4 kcal/mol; Table 2). Ge–H bond weakening is also responsible for the fact that, for the germanes, the formation of the radical pair occurs in an exothermic rather than slightly endothermic process ( $\Delta H_{\text{rad}}(\mathbf{1c}) = -8.3$ ;  $\Delta H_{\text{rad}}(\mathbf{1d}) = -7.5$  kcal/mol; Table 2). Again, this observation is only relevant to the solution rather than the gas phase. The final products (**2c** and **2d**, respectively) are formed in a less exothermic reaction ( $\Delta H_{\text{react}}(\mathbf{1c}) = -54.0$ ;  $\Delta H_{\text{react}}(\mathbf{1d}) = -63.7$  kcal/mol) than the corresponding Si products because of the reduced polarity of the Ge–O bond caused by the higher electronegativity of Ge.

In the gas phase, heterolytic Si–H (Ge–H) bond cleavage followed by the formation of the HOOO anion and a silylium or germylium cation is highly endothermic (Table 2). The corresponding data are included into Table 3 to obtain an estimate on solvent effects with regard to heterolytic bond cleavage. The effect of the solvent on the reaction mechanism was investigated by using a continuum dielectric solvent

**Table 3.** Reaction Energies for the Solvent-Phase-Optimized Ozonation of Silanes and Germanes (**1a–d**)<sup>a</sup>

molecule	$\Delta E$	$\Delta G$	$\mu$
<b>1a</b>	-517.29707	-517.28655	0, 0.62
<b>vdW1a</b>	0.47	1.31	1.03
<b>TS1(1a)</b>	11.22	9.82	1.28
H <sub>3</sub> Si <sup>+</sup> + HOOO <sup>-</sup>	34.66	34.90	0, 1.46
H <sub>3</sub> Si <sup>*</sup> + HOOO <sup>*</sup>	-0.99	-0.88	0.07, 1.47
<b>2a</b>	-77.11	-78.36	3.73
<b>1b</b>	-635.29002	-635.27341	0, 0.62
<b>vdW1b</b>	0.95	10.75	0.20
<b>TS1(1b)</b>	6.97	16.09	5.90
Me <sub>3</sub> Si <sup>+</sup> + HOOO <sup>-</sup>	8.81	7.15	0.01, 1.46
Me <sub>3</sub> Si <sup>*</sup> + HOOO <sup>*</sup>	-2.84	-3.11	0.87, 1.77
<b>2b</b>	-83.50	-75.52	4.61
<b>1c</b>	-231.59925	-231.58842	0, 0.62
<b>vdW1c</b>	3.98	4.97	0.96
<b>TS1(1c)</b>	11.33	10.50	2.67
H <sub>3</sub> Ge <sup>+</sup> + HOOO <sup>-</sup>	21.30	21.46	0, 1.46
H <sub>3</sub> Ge <sup>*</sup> + HOOO <sup>*</sup>	-10.92	-10.85	0, 1.47
<b>2c</b>	-61.94	-62.94	2.14
<b>1d</b>	-349.57192	-349.55470	0.65, 0.73
<b>vdW1d</b>	4.35	3.60	0.23
<b>TS1(1d)</b>	6.26	4.99	4.69
Me <sub>3</sub> Ge <sup>+</sup> + HOOO <sup>-</sup>	-1.12	-2.84	0, 1.46
Me <sub>3</sub> Ge <sup>*</sup> + HOOO <sup>*</sup>	-13.96	-14.24	0, 1.77
<b>2d</b>	-70.77	-72.95	2.72

<sup>a</sup> The energies and free energies are given in kcal mol<sup>-1</sup>. The dipole moment is in debye. All calculations were performed with B3LYP, and the 6-31G(d,p) basis set was used for all atoms except Ge, which was treated with the SDD pseudopotential. The CPCM solvent model was used with united force field atomic radii and the dielectric constant of acetone ( $\epsilon = 20.7$ ). For details, see the Supporting Information.

approach. The optimization of the structures, applying the dielectric constant of acetone ( $\epsilon = 20.7$ ), did not result in a change in the mechanism for the parent silane, **1a**. However, the TS geometry for the ozonation of **1a** changed from simultaneous H transfer and Si–O bond formation to late Si–O bond formation as observed already in the gas phase for **1b**, **1c**, and **1d**. This change is accompanied by a significant

(18) The SDD 28-electron pseudopotential and associated (4s,2p)/[3s,2p] basis set for the valence shell are used to describe the Ge atom; all other atoms are described with the 6-311++G(3df,3pd) basis set.

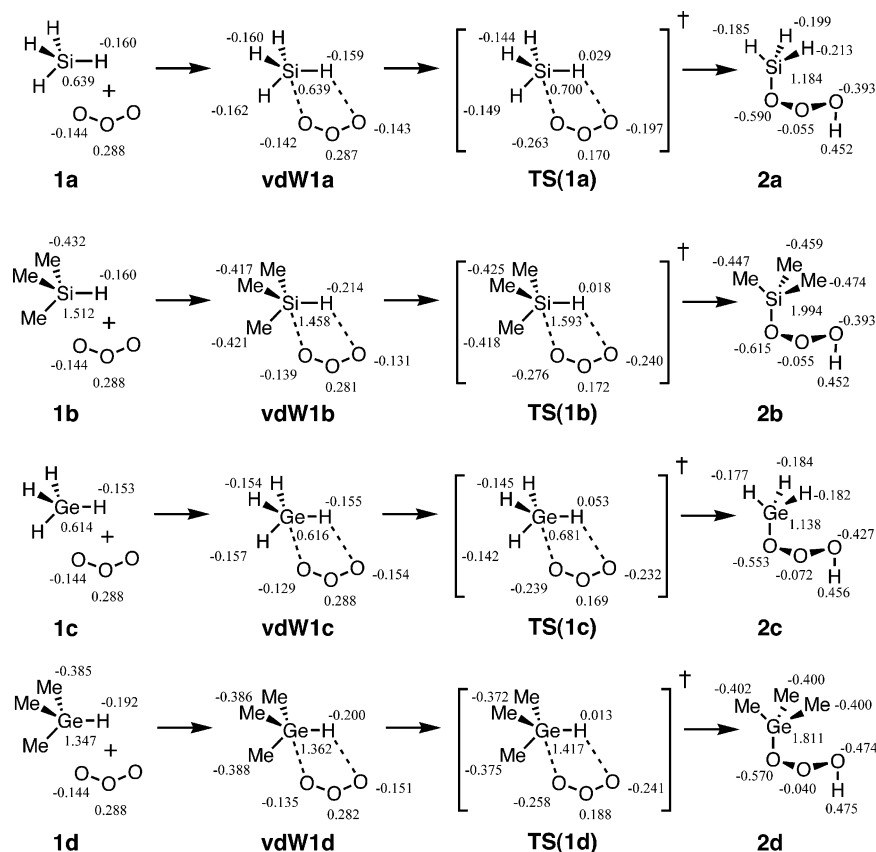


**Figure 4.** NBO partial charge distribution for the complexes involved in the ozonation of compounds **1a**–**d**. Charges for compounds **1a** and **1c** have been calculated with the 6-311++G(3df,3pd) basis set, whereas **1b** and **1d** were done with the 6-31G(d,p) basis set. All calculations employed the B3LYP hybrid functional. For structures containing the methyl groups, the charges of the methyl H atoms have been summed into the carbon. For details of the calculations, see the Supporting Information.

reduction of the free energy of activation leading to  $\Delta G_{\text{act}}^{\text{solv}} = 9.8$  kcal/mol (Table 3).

The change in the TS geometry opens the possibility of a solvent-supported shift from the concerted mechanism to a two-step process leading to an intermediate radical pair. Specific solvation of the reaction complex by one or more solvent molecules can separate  $\text{H}_3\text{Si}\cdot$  and  $\cdot\text{OOOH}$  so that they exist for a certain lifetime outside the solvent cage before abstracting H atoms from another partner, such as unreacted silane. At least part of  $\text{HOOOH}$  might be formed (beside the recombination product  $\text{H}_3\text{SiOOOH}$ ) in this way. The experimental results appear to suggest this possibility (observation of small amounts of  $\text{HOOOH}$  even before the decomposition of  $\text{R}_3\text{EOOOH}$ ), although our continuum description (specific solvation in the continuum) is not suitable for proving this reaction product.

We note that the concerted insertion mechanism when investigated with the URVA (unified reaction valley approach) of Kraka and co-workers<sup>19</sup> indicates for **1b**, **1c**, and **1d** in the gas phase a “hidden intermediate”. Such an intermediate does not correspond to a minimum (stationary point) on the potential energy surface, but is associated with an area of the reaction path distinctively differing from other path areas (TS area, vdW area, reactant area, product area). As found for symmetry forbidden addition reactions, such hidden intermediates indicate a change in the reaction mechanism from a concerted to a nonconcerted (two-step) mechanism under the impact of environmental factors (solvent polarity, added salt effect, etc.). Our

calculations confirm the existence of hidden intermediates, however, they do not give the conditions under which experimental conditions of a solvent-stabilized radical pair are generated.

Contrary to other ozone reactions,<sup>13</sup> the formation of an ion pair requires, even in acetone, a higher energy than the formation of a radical pair (in the case of **1a**,  $\Delta G_{\text{rad}}^{\text{solv}} = -0.9$  kcal/mol,  $\Delta G_{\text{ion}}^{\text{solv}} = 34.9$  kcal/mol; Table 3), where differences reach from 11 kcal/mol (methyl-substituted systems **1b** and **1d**) to more than 30 kcal/mol (**1c**, 32.3; **1a**, 35.8 kcal/mol; Table 3), despite the stabilizing influence of the solvent on the ionic pair. In the methyl-substituted ions, charge polarization is much larger than in the parent compounds (as is already reflected by the NBO charges of the TSs given in Figure 4), and accordingly, the relative energies of the ions in acetone are closer to those of the radicals. Considering that heterolytic cleavage is facilitated by acetone by more than 100 kcal/mol, one can predict that a more polar solvent than acetone can stabilize a potential ion pair to such an extent that its stability becomes comparable with that of a radical pair.

The overall reaction mechanism for the germanes remains unaffected by the inclusion of solvent effects, although there is a shift in the relative energies. The activation free energy is reduced in both **1c** and **1d** by more than 10 kcal/mol ( $\Delta G_{\text{act}}^{\text{solv}}(\mathbf{1c}) = 10.5$ ;  $\Delta G_{\text{act}}^{\text{solv}}(\mathbf{1d}) = 5.0$  kcal/mol; Table 3). We note that a potential generation of radical pairs is more exothermic in acetone than in the gas phase ( $\Delta G_{\text{rad}}^{\text{solv}}(\mathbf{1c}) = -10.9$ ;  $\Delta G_{\text{rad}}^{\text{solv}}(\mathbf{1d}) = -14.2$  kcal/mol; Table 3).

(19) Cremer, D.; Wu, A.; Kraka, E. *Phys. Chem. Chem. Phys.* **2001**, *3*, 674.

**Table 4.** Kinetic and Activation Parameters for the Decomposition of Hydrotrioxides (ROOOH, **2**) and Dihydrogen Trioxide (HOOOH), Formed in the Low-Temperature Ozonation of Trimethylsilane (**1b**), Triethylsilane (**1e**), Dimethylphenylsilane (**1f**), Triphenylsilane (**1g**), Triethylgermane (**1h**), and Dimethylphenylgermane (**1i**) in Various Solvents<sup>a</sup>

solvent	T, °C	ROOOH				HOOOH				
		δ, ppm ROOOH	k × 10 <sup>4</sup> , s <sup>-1</sup> OOOH <sup>b</sup>	k × 10 <sup>4</sup> , s <sup>-1</sup> CH <sub>3</sub> <sup>c</sup>	E <sub>a</sub> , kcal mol <sup>-1</sup>	log A	δ, ppm	k × 10 <sup>4</sup> , s <sup>-1</sup>	E <sub>a</sub> , kcal mol <sup>-1</sup>	log A
( <b>2b</b> ) acetone-d <sub>6</sub>	-40	13.43	12.3		(10.0 ± 1.0) <sup>b</sup>	(6.3 ± 0.7) <sup>b</sup>	13.15	1.45	(11.0 ± 2.0)	(6.1 ± 1.0)
methyl acetate	-40	12.88	0.47	0.46	(11.9 ± 1.2) <sup>b</sup>	(7.0 ± 0.8) <sup>b</sup>	12.63	0.88	(13.8 ± 1.5)	(8.7 ± 0.9)
tert-butyl methyl ether	-20	12.70	4.46	4.34	(11.9 ± 1.2) <sup>c</sup>	(6.9 ± 0.7) <sup>c</sup>	12.45	4.57		
tert-butyl methyl ether	-40	13.30	1.10		(11.7 ± 1.3) <sup>b</sup>	(7.3 ± 0.8) <sup>b</sup>	12.95			
( <b>2e</b> ) acetone-d <sub>6</sub>	-40	13.57	1.80	2.40	(9.3 ± 1.1) <sup>b</sup>	(5.0 ± 0.6) <sup>b</sup>	13.27			
methyl acetate	-20	13.39	7.33	6.80	(8.9 ± 1.0) <sup>c</sup>	(4.6 ± 0.6) <sup>c</sup>	13.10			
tert-butyl methyl ether	-40	13.02	0.37	0.34	(14.5 ± 1.2) <sup>b</sup>	(9.3 ± 0.9) <sup>b</sup>				
methylene chloride-d <sub>2</sub>	-20	12.78	4.94	3.86	(14.4 ± 1.2) <sup>c</sup>	(9.1 ± 0.9) <sup>c</sup>				
toluene-d <sub>8</sub>	-40	13.16	0.32		(10.8 ± 1.1) <sup>b</sup>	(5.7 ± 0.6) <sup>b</sup>				
tert-butyl methyl ether	-20	13.02	1.94							
methylene chloride-d <sub>2</sub>	-70	13.84	3.53	3.37	(12.8 ± 1.1) <sup>b</sup>	(10.4 ± 0.9) <sup>b</sup>				
toluene-d <sub>8</sub>	-60	13.72	22.5	19.3	(12.7 ± 1.1) <sup>c</sup>	(10.3 ± 0.9) <sup>c</sup>				
tert-butyl methyl ether	-70	12.10	0.30	0.24	(14.2 ± 1.2) <sup>b</sup>	(10.7 ± 1.0) <sup>b</sup>				
acetone-d <sub>6</sub>	-60	11.35	1.24	0.97	(14.3 ± 1.2) <sup>c</sup>	(10.7 ± 1.0) <sup>c</sup>				
( <b>2f</b> ) acetone-d <sub>6</sub>	-40	13.56	3.70		(9.5 ± 1.0) <sup>b</sup>	(5.5 ± 0.7) <sup>b</sup>	13.16	0.56	(11.0 ± 2.0)	(6.1 ± 1.0)
methyl acetate	-40	13.24	2.70		(10.0 ± 1.1) <sup>b</sup>	(5.9 ± 0.7) <sup>b</sup>	12.85			
tert-butyl methyl ether	-20	13.02	17.0				12.63			
tert-butyl methyl ether	-40	13.30	1.45		(12.6 ± 1.1) <sup>b</sup>	(8.2 ± 0.8) <sup>b</sup>	12.79			
( <b>2g</b> ) acetone-d <sub>6</sub>	-40	14.00	4.91		(11.8 ± 1.1) <sup>b</sup>	(7.8 ± 0.8) <sup>b</sup>				
tert-butyl methyl ether	-40	13.49	12.37		(10.9 ± 1.2) <sup>b</sup>	(7.4 ± 0.8) <sup>b</sup>	12.75			
( <b>2h</b> ) acetone-d <sub>6</sub>	-40	13.05	0.41		(10.5 ± 1.2) <sup>b</sup>	(5.4 ± 0.7) <sup>b</sup>	13.31			
methyl acetate	10						12.84	6.24	(16.1 ± 1.0)	(9.4 ± 0.7)
tert-butyl methyl ether	-40	12.65	0.91		(10.6 ± 1.2) <sup>b</sup>	(5.8 ± 0.7) <sup>b</sup>	12.88	0.88	(13.8 ± 1.5)	(8.7 ± 0.7)
tert-butyl methyl ether	-20	12.42	3.75				12.67	8.10		
tert-butyl methyl ether	-20	12.57	1.17		(12.7 ± 1.1) <sup>b</sup>	(7.1 ± 0.6) <sup>b</sup>	12.64			
tert-butyl methyl ether	10						12.74	1.57	(12.0 ± 1.6)	(5.4 ± 0.6)
( <b>2i</b> ) acetone-d <sub>6</sub>	-40	13.16	3.24	3.00	(9.0 ± 1.5) <sup>b</sup>	(5.0 ± 0.6) <sup>b</sup>	13.29			
methyl acetate	10				(8.9 ± 1.5) <sup>c</sup>	(4.9 ± 0.7) <sup>c</sup>	12.83	2.70	(11.9 ± 1.5)	(5.6 ± 0.6)
tert-butyl methyl ether	-40	12.56	0.74	0.62	(12.7 ± 1.3) <sup>b</sup>	(7.8 ± 0.6) <sup>b</sup>	12.72			
tert-butyl methyl ether	10				(13.2 ± 1.2) <sup>c</sup>	(8.2 ± 0.7) <sup>c</sup>	12.27	1.07	(12.6 ± 1.6)	(5.9 ± 0.6)
tert-butyl methyl ether	-40	12.86	3.52		(7.4 ± 2.0) <sup>b</sup>	(3.2 ± 1.2) <sup>b</sup>	12.78			
tert-butyl methyl ether	20						12.39	0.71	(17.2 ± 0.5)	(8.9 ± 0.8)

<sup>a</sup> **1** = (0.10 ± 0.05) M, **2** = (0.09 ± 0.05) M, HOOOH = (0.05 ± 0.02) M. Standard deviation ±10%. <sup>b</sup> Following decay of the OOOH absorption by <sup>1</sup>H NMR spectroscopy. <sup>c</sup> Following decay of the CH<sub>3</sub> absorption by <sup>1</sup>H NMR spectroscopy.

**The Decomposition of Silyl and Germyl Hydrotrioxides.** Hydrotrioxides of silanes (**2e–g**) decomposed in the temperature range of -85 to -10 °C to produce the corresponding silanols (94 ± 3%, yield/mol of **2**), disiloxanes (4 ± 2%), and singlet oxygen, O<sub>2</sub>(<sup>1</sup>Δ<sub>g</sub>) (70 ± 10%), as revealed by GC/MS method, <sup>1</sup>H NMR spectroscopy, and 9,10-dimethylanthracene as singlet oxygen acceptor.<sup>1a,4,20</sup> Hydrogen peroxide was also detected as a minor product in the decomposition mixture (5 ± 2% yield by iodometry) after the warm-up procedure. It is interesting to mention that smaller amounts of trimethylsilanol (40 ± 10%, yield/mol of **1b**) and larger amounts of hexamethyldisiloxane (60 ± 10%) were detected after the decomposition of trimethylsilyl hydrotrioxide (**2b**). Similarly, the corresponding digermoxanes were found as the main decomposition products (85 ± 5%) after the decomposition of germyl hydrotrioxides (**2h–i**).

Besides the decomposition products already mentioned, dihydrogen trioxide (HOOOH) was formed (40 ± 20%, yield/

mol of **2**) during the decomposition of all investigated hydrotrioxides (**2**). We also noticed that the amount of the HOOOH formed was larger when the warm-up was slower. Additionally, we observed significantly larger amount of HOOOH formed (80 ± 10%, yield/mol of **2**) when water was added to the solutions of **2** in all solvents investigated. A relatively faster decomposition of **2f** in acetone-d<sub>6</sub> with added water was observed (compare with Tables 4 and S3 in Supporting Information). Similarly, the addition of CH<sub>3</sub>OH or (CH<sub>3</sub>)<sub>3</sub>SiOH to the ozonized solution of silanes (**1b,e,f**) in acetone-d<sub>6</sub> leads to the formation of larger amounts of HOOOH and, at the same time, the formation of either methoxy-substituted silane or mixed disiloxane, respectively.

**Kinetic Studies.** The kinetics of decomposition of the hydrotrioxides **2** was measured by following the decay of OOOH and CH<sub>3</sub> absorptions by <sup>1</sup>H NMR spectroscopy and was found to obey first-order kinetics in all solvents investigated. Both absorptions decayed by approximately the same rate. The kinetic and activation parameters for the decomposition of **2** in various solvents are summarized in Table 4 (see also Tables S1 and S2 in Supporting Information). The disappearance of the O–H and O–O stretching frequencies in the IR spectra of

(20) It should be pointed out that singlet oxygen is formed in the ozonation of various organic compounds. See, for example: (a) Munoz, F.; Mvula, E.; Braslavsky, S. E.; von Sonntag, C. *J. Chem. Soc., Perkin Trans. 2* **2001**, 1109, and references therein. (b) For older literature, see: Plesničar, B. In *Organic Peroxides*; Ando, W., Ed.; Wiley & Sons: New York, 1992; p 479.

triethylsilyl hydrotrioxide (**2e**) is shown in Figure S2 (Supporting Information).

The effect of solvent polarity and basicity on the decomposition of the hydrotrioxides **2** was also examined. We found that the rate of decomposition of **2** is only slightly sensitive to solvent polarity, the rate increasing with the solvent polarity (**2e**:  $k_{\text{rel}}(-40\text{ }^\circ\text{C}) = 1.80, 0.37, \text{ and } 0.32$  for acetone- $d_6$ , methyl acetate, and *tert*-butyl methyl ether, respectively) and the amount of water present in the reaction mixture (molar ratio  $2/\text{H}_2\text{O} = 1:2$  in acetone- $d_6$  (by  $^1\text{H NMR}$ )). Namely, water was always present in the reaction mixture in sufficient amounts to participate in the reaction. Furthermore, the addition of water (2 vol %) to acetone- $d_6$  solutions did not change significantly the activation parameters of the decomposition of **2** (compare Tables 4 and S3).

The involvement of water in the decomposition was also confirmed by the magnitude of the solvent isotope effect for the decomposition of **2f**, that is,  $k_{\text{H}_2\text{O}}/k_{\text{D}_2\text{O}} = 1.65 \pm 0.20$ , and HOOH ( $k_{\text{H}_2\text{O}}/k_{\text{D}_2\text{O}} = 4.5 \pm 0.7$ ), which indicated a considerable water-assisted proton transfer in the transition state of this reaction (see also Table S3 in Supporting Information).

Only small amounts (sometimes below the detection limit<sup>21</sup>) of HOOH was formed during the decomposition of hydrotrioxides **2** in methylene chloride- $d_2$  and toluene- $d_8$ , most probably due to the low solubility of water in these solvents. Again, this observation supports the involvement of water in proton transfer processes during the formation of dihydrogen trioxide.

**Mechanism of the Decomposition Reactions.** The primary focus of the theoretical investigation on the decomposition of **2a–d** was to establish plausible mechanisms that describe this process and result in the experimentally observed products. As observed in the experimental studies, the final products of these reactions should include dihydrogen trioxide (HOOH), silanols/germanols (**5a–d**), and disiloxanes/digermoxanes (**4a–d**). The generation of HOOH was detected in the reaction mixture in appreciable amounts, and therefore, we considered, beside the direct formation in the first step via radical formation, also other mechanisms, by which the formation of this species could occur (paths A, B, and C, Scheme 2). Paths A, B, and C would also lead to disilyl/digermyl trioxide (**3a–d**), disiloxane/digermoxane (**4a–d**) and silanol/germanol (**5a–d**) depending on what reaction partner **2a–d** would find in the reaction mixture (a second hydrotrioxide, silanol (germanol), and water). In each of these cases, water would play a catalytic role. Calculated results describing the energetics associated with paths A, B, and C are listed in Table 5.

As for path A, both **2a** and **2c** are found to react with moderate activation enthalpies ( $\Delta H_{\text{act}}(\mathbf{2a}) = 16.5$ ;  $\Delta H_{\text{act}}(\mathbf{2c}) = 13.9$  kcal/mol). However, the TSs for the substituted compounds (TS(**2b–3b**) and TS(**2d–3d**)) could not be located on the potential energy surface probably because steric hindrance excludes an energetically favorable approach of the reaction partners. Therefore, it is not likely that this mechanism could be active for the more highly substituted compounds tested experimentally. A mechanistic modification of this reaction without the additional water molecule was also tested for **2a**;

however, the calculated activation enthalpy for this reaction is too large ( $\Delta H_{\text{act}}(\mathbf{2a}) = 29.2$  kcal/mol) to warrant further investigation of this mechanism for the other species.

Path B involves the use of a silanol/germanol molecule that results from an alternative decomposition mechanism. As in the case of path A, the calculated activation enthalpies for the parent compounds **2a** and **2c** are both within the experimental limit ( $\Delta H_{\text{act}}(\mathbf{2a}) = 13.7$ ;  $\Delta H_{\text{act}}(\mathbf{2c}) = 11.9$  kcal/mol), whereas the activation enthalpies for **2b** ( $\Delta H_{\text{act}} = 29.1$  kcal/mol) and **2d** ( $\Delta H_{\text{act}} = 19.8$  kcal/mol) are again too large. All path B reactions are calculated to be mildly exothermic ( $\Delta H_{\text{react}} \approx -5$  kcal/mol). As in the case of path A, it is the steric bulk of the methyl groups that hinders the approach of the silanol/germanol and consequently results in larger activation barriers.

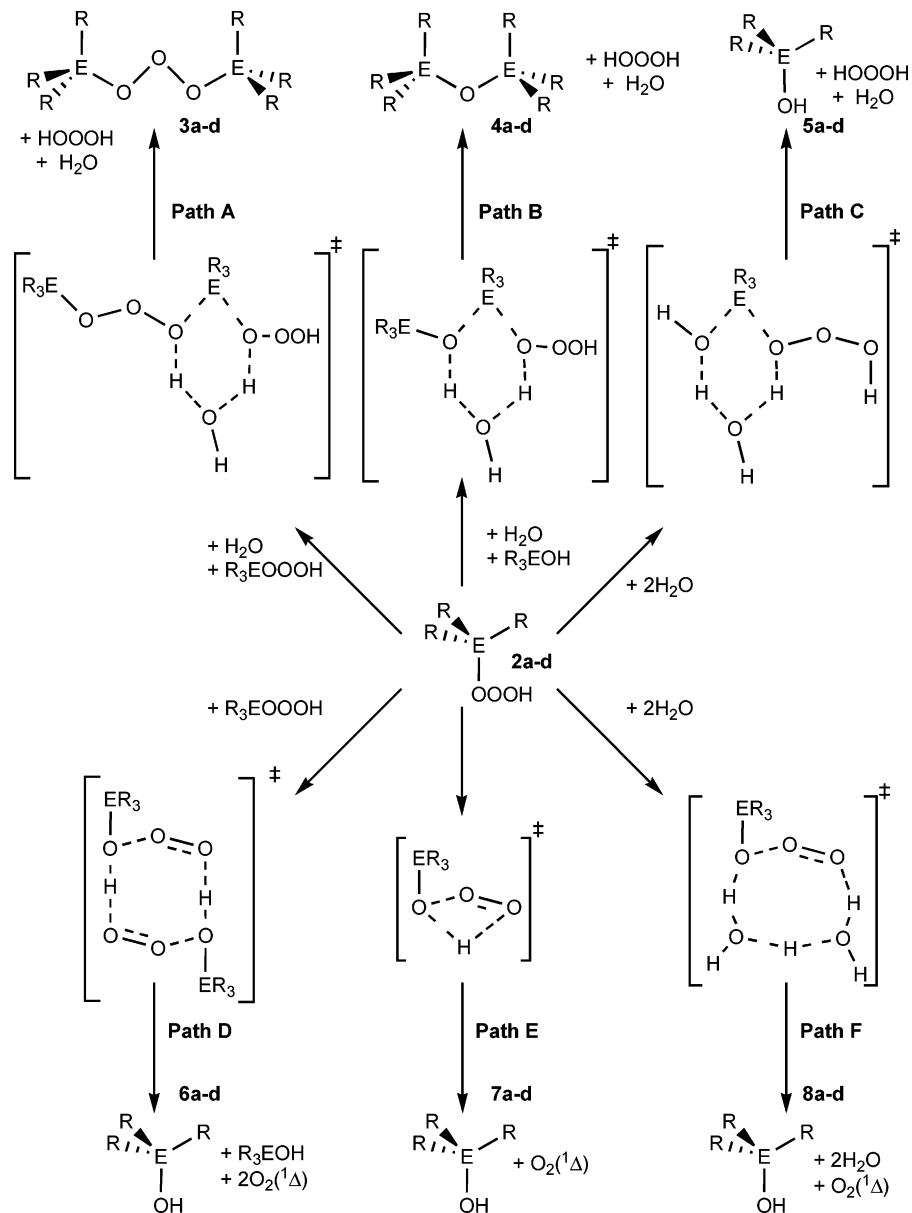
In the case of path C, first a single water variant was tested; however, the activation barriers for all four species (**2a–d**) were too large (e.g.,  $\Delta H_{\text{act}}(\mathbf{2b}) = 29.2$  kcal/mol;  $\Delta H_{\text{act}}(\mathbf{2d}) = 21.4$  kcal/mol) to explain the experimentally observed formation of HOOH. The high barriers result primarily from the strain in the four-membered cyclic TS involving the Si–O(OOH) bond and the H–O(H) bond of the water molecule. Therefore, we tested the two-water mechanism shown as path C. This leads to activation enthalpies of 10.5, 22.6, 13.1, and 20.0 kcal/mol respectively, reflecting the steric advantages of a six-membered pericyclic arrangement. Despite the favorable reduction in the activation enthalpy, the barriers calculated for **2b** and **2d** are still too large, again due to the steric repulsion with the methyl groups, to explain the observed HOOH formation.

Three alternative decomposition pathways that may also account for this formation are shown, namely, paths D, E, and F (Scheme 2). Path D involves the possible decomposition of two hydrotrioxide species to two silanol/germanol molecules and  $\text{O}_2(^1\Delta_g)$  (**6a–d**, Scheme 2) in an exothermic reaction ( $\Delta H_{\text{react}}(\mathbf{6a}) = -22.9$ ;  $\Delta H_{\text{react}}(\mathbf{6b}) = -25.8$ ;  $\Delta H_{\text{react}}(\mathbf{6c}) = -9.9$ ;  $\Delta H_{\text{react}}(\mathbf{6d}) = -15.0$  kcal/mol; Table 5). The activation enthalpies for the four compounds are similar ( $\Delta H_{\text{act}} = 16\text{--}18$  kcal/mol), which reflects the fact that the interaction between the two hydrotrioxide molecules involves only their OOH units. The activation enthalpy of  $>15$  kcal/mol is too high to explain the occurrence of either  $\text{R}_3\text{EOH}$  or  $\text{O}_2(^1\Delta_g)$  under the experimental conditions.

Path E involves the intramolecular transfer of the hydrotrioxide H atom from O3 to O1, resulting in the formation of  $\text{O}_2(^1\Delta_g)$  and the silanol/germanol (**7a–d**). The investigation of this reaction path for the parent silane (**2a**) and germane (**2c**) reveals this mechanism to be an unlikely contributor to the decomposition of **2a–d** ( $\Delta H_{\text{act}}(\mathbf{2a}) = 39.2$ ;  $\Delta H_{\text{act}}(\mathbf{2c}) = 38.5$  kcal/mol). The large activation energy for this process is not unprecedented, with a similar mechanism for the parent dihydrogen trioxide species reportedly requiring an activation energy of  $48 \pm 2$  kcal/mol.<sup>1c</sup>

The final mechanism (path F), again, similar to path C, involves two water molecules as a catalyst for the formation of the silanol/germanol; however, in path F, both water molecules are retained and one molecule of  $\text{O}_2(^1\Delta_g)$  is formed (**8a–d**, Scheme 2). Initially, the single water analogue of path F was tested, resulting in moderate activation enthalpies, ranging from 17 to 20 kcal/mol across the series. However, these activation enthalpies were still too high, compared to that which was obtained experimentally. Thus, we considered path F (the two-

(21) The OOH absorption of all polyoxides under investigation is very broad in methylene chloride and toluene. Addition of small amounts of an oxygen base (acetone, ethers) to such solutions considerably sharpens this absorption.

**Scheme 2.** Possible Decomposition Paths for **2a**, **2b**, **2c**, and **2d** (E = Si, Ge; R = H, Me)

water mechanism) to test whether a lowering of the strain in the cyclic TS (Scheme 2) would help to lower the activation enthalpy. Indeed, this was observed with a decrease in all cases by about 5 kcal/mol. This leads to an activation enthalpy of 12.7 kcal/mol for **2b** and 14.4 kcal/mol for **2d**, which are both comparable with the measured activation enthalpy for the decomposition of these species. Additionally, the products **8a-d** were found to be generated in an exothermic reaction, where a reaction enthalpy of  $-12$  to  $-15$  kcal/mol ( $\Delta H_{\text{react}}(\mathbf{2b}) = -13.4$ ;  $\Delta H_{\text{react}}(\mathbf{2d}) = -12.5$  kcal/mol) was calculated.

Thus, we conclude that the formation of the silanol and germanol species occurs via the two-water-catalyzed mechanism (path F) and results in the formation of O<sub>2</sub>(<sup>1</sup>Δ<sub>g</sub>), which was also detected experimentally. This mechanism of decomposition is expected to be the primary source of the O<sub>2</sub>(<sup>1</sup>Δ<sub>g</sub>) and the R<sub>3</sub>EOH detected in the reaction mixture.

#### Spectroscopic Characterization of Silyl Hydrotrioxides.

Dihydrogen trioxide (HOOH)<sup>2d</sup> and alkyl hydrotrioxides have been previously characterized by both NMR spectroscopy and

quantum chemical calculations.<sup>22</sup> All silyl and germyl hydrotrioxides under investigation (except for dimethylphenylsilyl hydrotrioxide) were characterized by IR and NMR spectroscopy in this work for the first time, and our calculations in combination with the measured data (Table 1) clearly reveal that <sup>17</sup>O NMR spectroscopy is the appropriate tool to detect and identify these hydrotrioxides (see part 4 of the Supporting Information). The IR spectra of the hydrotrioxides **2** (in solutions) are reported for the first time, whereas their analysis based on the adiabatic mode approach provides an insight into the electronic structure of these compounds (see Supporting Information). The previous matrix IR study of the reaction of ozone with the parent silane (**1a**) and trimethylsilane (**1b**), reported by Andrews et al.,<sup>23</sup> did not reveal the presence of the corresponding hydrotrioxides **2a** and **2b**. For a discussion of their IR spectra, see part 4 of the Supporting Information.

(22) Wu, A.; Cremer, D.; Gauss, A. *J. Phys. Chem. A* **2003**, *107*, 8737.

(23) Withnall, R.; Andrews, L. *J. Phys. Chem.* **1988**, *92*, 594.

**Table 5.** Reaction Energies for the Decomposition of Silyl and Germyl Hydrotrioxides (**2a–d**)<sup>a</sup>

molecule	$\Delta E$	$\Sigma ZPE$	$\Delta H$	$\Sigma S$	$\Delta G$	$\mu$	B.E.
Path A							
<b>2a</b>	-1111.27411	74.32	-1111.13854	137.18	-1111.20372	4.17	-13.47
<b>TS(2a–3a)</b>	19.44	73.13	16.46	115.43	22.95	2.70	
<b>3a</b>	-0.19	74.38	-0.19	131.40	1.53	3.73	-13.14
<b>2c</b>	-539.82166	70.66	-539.69115	145.26	-539.76017	4.24	-14.50
<b>TS(2c–3c)</b>	17.38	68.86	13.91	123.40	20.43	3.27	
<b>3c</b>	-2.35	70.87	-2.24	138.23	-0.14	5.39	-16.57
Path B							
<b>2a</b>	-961.01205	70.01	-960.88562	123.64	-960.94437	3.09	-13.81
<b>TS(2a–4a)</b>	16.83	68.67	13.67	103.38	19.70	3.02	
<b>4a</b>	-6.46	70.66	-5.83	121.49	-5.19	1.59	-11.28
<b>2b</b>	-1197.01811	178.44	-1196.70913	166.56	-1196.78827	3.65	-14.07
<b>TS(2b–4b)</b>	31.18	177.19	29.05	155.38	32.38	2.24	
<b>4b</b>	-6.23	179.07	-5.17	168.76	-5.82	2.10	-12.92
<b>2c</b>	-389.55710	66.68	-389.43543	132.27	-389.49828	2.67	-14.84
<b>TS(2c–4c)</b>	15.61	64.27	11.91	115.65	16.86	4.12	
<b>4c</b>	-6.02	67.10	-5.77	125.29	-3.69	2.72	-17.76
<b>2d</b>	-625.53184	176.81	-625.22392	177.31	-625.30816	3.28	-15.30
<b>TS(2d–4d)</b>	20.59	176.56	19.78	168.93	22.27	2.96	
<b>4d</b>	-4.73	177.53	-3.84	176.33	-3.55	3.11	-19.58
Path C							
<b>2a</b>	-670.27984	60.98	-670.17079	102.12	-670.21931	2.11	-16.49
<b>TS(2a–5a)</b>	14.01	58.88	10.50	90.65	13.92	3.61	
<b>5a</b>	-11.40	61.04	-11.28	104.24	-11.91	0.53	-18.52
<b>2b</b>	-788.28412	114.32	-788.08381	131.61	-788.14634	2.84	-13.52
<b>TS(2b–5b)</b>	26.14	112.61	22.59	115.91	27.27	3.35	
<b>5b</b>	-7.10	114.82	-6.84	133.32	-7.35	2.72	-15.78
<b>2c</b>	-384.55242	58.86	-384.44614	106.59	-384.49679	2.02	-15.31
<b>TS(2c–5c)</b>	16.79	56.37	13.09	97.43	15.82	3.82	
<b>5c</b>	-4.50	58.93	-4.26	112.48	-6.01	2.80	-16.18
<b>2d</b>	-502.54218	113.57	-502.34241	136.61	-502.40732	3.19	-16.16
<b>TS(2d–5d)</b>	23.35	111.62	19.99	125.89	23.19	4.45	
<b>5d</b>	-4.89	114.18	-4.59	137.83	-4.96	2.93	-18.78
Path D							
<b>2a</b>	-1034.85001	59.08	-1034.74222	115.94	-1034.79730	0	-11.15
<b>TS(2a–6a)</b>	21.42	53.94	15.87	112.15	16.99	0	
<b>6a</b>	-21.26	56.48	-22.90	124.26	-25.38	1.44	-17.57
<b>2b</b>	-1270.85766	167.34	-1270.56717	162.40	-1270.64433	0.01	-12.38
<b>TS(2b–6b)</b>	22.33	53.94	17.45	112.15	16.57	0.00	
<b>6b</b>	-25.30	56.48	-25.79	124.26	-31.24	1.44	-8.03
<b>2c</b>	-463.40309	55.85	-463.30006	120.14	-463.35714	0.00	-14.47
<b>TS(2c–6c)</b>	22.88	53.94	17.84	112.15	18.25	0.00	
<b>6c</b>	-9.07	56.48	-9.94	124.26	-13.72	1.44	-7.14
<b>2d</b>	-699.37983	166.19	-699.08926	174.99	-699.17240	0.01	-15.93
<b>TS(2d–6d)</b>	22.92	53.94	18.44	112.15	19.21	0.00	
<b>6d</b>	-14.07	56.48	-15.02	124.26	-18.97	1.44	-15.02
Path E							
<b>2a</b>	-517.41073	28.78	-517.35814	75.07	-517.39381	2.90	
<b>TS(2a–7a)</b>	43.16	24.89	39.22	74.98	39.25	3.07	
<b>7a</b>	-18.66	27.18	-19.07	91.69	-24.02	1.90	-1.76
<b>2c</b>	-231.68862	26.92	-231.63857	79.35	-231.67627	1.59	
<b>TS(2c–7c)</b>	42.07	23.51	38.49	78.37	38.78	4.86	
<b>7c</b>	-14.44	25.48	-14.76	95.12	-19.46	1.88	-1.26
Path F							
<b>2a</b>	-670.29860	60.84	-670.18972	102.69	-670.23851	1.72	-22.81
<b>TS(2a–8a)</b>	16.38	56.71	11.27	95.61	13.38	3.63	
<b>8a</b>	-13.98	59.64	-14.50	109.32	-16.48	2.19	-21.63
<b>2b</b>	-788.30149	115.02	-788.10079	129.34	-788.16224	2.14	-22.64
<b>TS(2b–8b)</b>	18.22	110.53	12.72	122.34	14.81	2.67	
<b>8b</b>	-12.87	113.86	-13.42	135.95	-15.39	1.43	-20.90
<b>2c</b>	-384.57074	59.16	-384.46421	107.13	-384.51511	2.58	-22.44
<b>TS(2c–8c)</b>	19.16	54.53	13.48	98.39	16.09	2.77	
<b>8c</b>	-13.31	58.39	-13.62	110.47	-14.62	1.78	-22.07
<b>2d</b>	-502.55841	114.34	-502.35810	136.04	-502.42273	3.07	-22.71
<b>TS(2d–8d)</b>	20.42	109.32	14.37	127.61	16.89	3.12	
<b>8d</b>	-12.07	113.36	-12.51	142.53	-14.45	2.05	-21.89

<sup>a</sup> The energies, enthalpies, free energies, and binding energies (B.E. = basis set superposition error is corrected) are given in kcal mol<sup>-1</sup>. The entropy is in e.u., and the dipole moment is in debye. All calculations were performed with B3LYP, and the 6-31G(d,p) basis set was used for all atoms except Ge, which was treated with the SDD pseudopotential. For details of the calculations, see the Supporting Information.

## Conclusions

In the present investigation, we have demonstrated that the ozonation of various silanes and germanes produced the corresponding hydrotrioxides,  $R_3SiOOOH$  and  $R_3GeOOOH$ , which were characterized by  $^1H$ ,  $^{13}C$ ,  $^{17}O$ , and  $^{29}Si$  NMR, and (for the first time for any polyoxide) by IR spectroscopy. Calculated NMR chemical shifts and characteristic IR frequencies in acetone- $d_6$  as solvent agree well with the experimentally obtained values.

A theoretical investigation of the first step of the ozonation reaction (i.e., the formation of the hydrotrioxides) revealed that a concerted 1,3-dipolar insertion mechanism, proposed in the past to accommodate the experimental data, is operative for all compounds investigated in the gas phase. However, in substituted silanes and all germanes as well as in acetone- $d_6$  solutions, the H atom transfer increasingly precedes the E–O formation. Considering dynamic effects (not investigated in this work), one cannot exclude that the formation of a radical pair,  $R_3E^{\bullet}OOH$ , encompassed in a solvent cage is possible. Collapsing of the radical pair would lead to a hydrotrioxide ( $R_3EOOOH$ ), whereas diffusion out of the solvent cage would be the first step for  $HOOOH$  generation.

The hydrotrioxides under investigation decompose in acetone- $d_6$ , methyl acetate, and *tert*-butyl methyl ether into the corresponding silanols/germanols, disiloxanes/digermoxanes, singlet oxygen ( $O_2(^1\Delta_g)$ ), and dihydrogen trioxide ( $HOOOH$ ). The activation parameters for the decomposition of the hydrotrioxides, together with the magnitude of the kinetic solvent effect indicate the involvement of water in these reactions. Several mechanistic possibilities for the formation of all these products were tested. Theoretical results indicate that there are at least two competing reactions, both first-order processes, which can accommodate all the decomposition products. The first one, involving the cleavage of the  $R_3EOOOH$  bond with the formation of  $R_3EOH$  and  $O_2(^1\Delta_g)$ , is assisted by two molecules of water. This mechanistic pathway has the lowest activation energy and is most likely operative in “inert” solvents, such as  $CH_2Cl_2$ , in which water is only sparingly soluble.

Competing with this path is the cleavage of the  $R_3EOOOH$  bond to yield  $R_3EOH$  and  $HOOOH$ , which is also assisted by two molecules of water. Because water was always present in the reaction mixture, this mechanistic pathway appears to be more important in acetone- $d_6$  (and methyl acetate or *tert*-butyl methyl ether) than in methylene chloride- $d_2$ , due to the different solubility of water in these solvents. A relatively high activation enthalpy of the reactions, as compared to the experimentally obtained values, appears to indicate that even greater assemblies of water molecules (most likely assisted by one or more molecules of  $R_3EOH$ , and perhaps acetone as well) might be involved in these decompositions.

The formation of dihydrogen trioxide ( $HOOOH$ ) in the decomposition of organometallic hydrotrioxides in acetone- $d_6$  represents a new and convenient method for the preparation of this simplest of polyoxides. When run in methylene chloride as solvent, these reactions (for example, the decomposition of  $Et_3SiOOOH$ ) are at present the method of choice for the generation of singlet oxygen ( $O_2(^1\Delta_g)$ ).

**Acknowledgment.** We dedicate this work to the memory of Professor Christopher (“Chris”) S. Foote, one of the pioneers in the field of singlet oxygen chemistry. At Ljubljana, this work was financially supported by the Slovenian Research Agency. D.C. and E.K. thank the University of the Pacific for generous support of their work. J.C. and B.P. thank Dr. Janez Plavec (Slovenian NMR Centre, National Institute of Chemistry, Ljubljana) for running  $^{17}O$  NMR spectra on the 600 MHz Varian spectrometer, and Prof. Janez Levec for enabling the low-temperature IR measurements.

**Supporting Information Available:** Instrumentation, materials, ozonation procedures, product analysis, methodology of kinetic studies, energy data, and the analysis of the calculated and measured NMR and IR spectra are provided (38 pages, PDF). The geometries of all calculated structures, reported in this work, are also available in xyz format (TXT). This material is available free of charge via the Internet at <http://pubs.acs.org>.

JA058065V